

# The probability of mantle plumes in global tomographic models

Augustin Marignier<sup>1,2,\*</sup>, Ana MG Ferreira<sup>2,3</sup>, and Thomas Kitching<sup>1</sup>

<sup>1</sup>Mullard Space Science Laboratory, UCL, UK <sup>2</sup>Department of Earth Sciences, UCL, UK <sup>3</sup>Instituto Superior Técnico, Universidade de Lisboa, Portugal

\*augustin.marignier.14@ucl.ac.uk



## Introduction

Mantle plumes are notoriously difficult to resolve in seismic tomography, and with a general lack of full uncertainty quantification, it is difficult to assess the robustness of features in models. As such, models are generally assessed visually, but an automated numerical assessment is required to quantify the presence of features objectively (e.g. Lekic et al. (2012), Cottaar and Lekic (2016)). In this work we use a spherical wavelet transform to simulate the noise in 6 tomographic models and assess the probability that plumes are robust features, and not noise or artefacts of the model construction.

## Spherical Wavelet Transform

The wavelet transform is like a Fourier transform, but it keeps the localisation information as well as the frequency (Figure 1b-j). Using the wavelet transform we can separate out the small-scale signals of a tomographic model, and simulate them as if they were random noise. Taking the inverse transform we recover a new version of the model (Figure 1k). We repeat this process to obtain a large sample, on which we can perform some statistical tests about plumes.

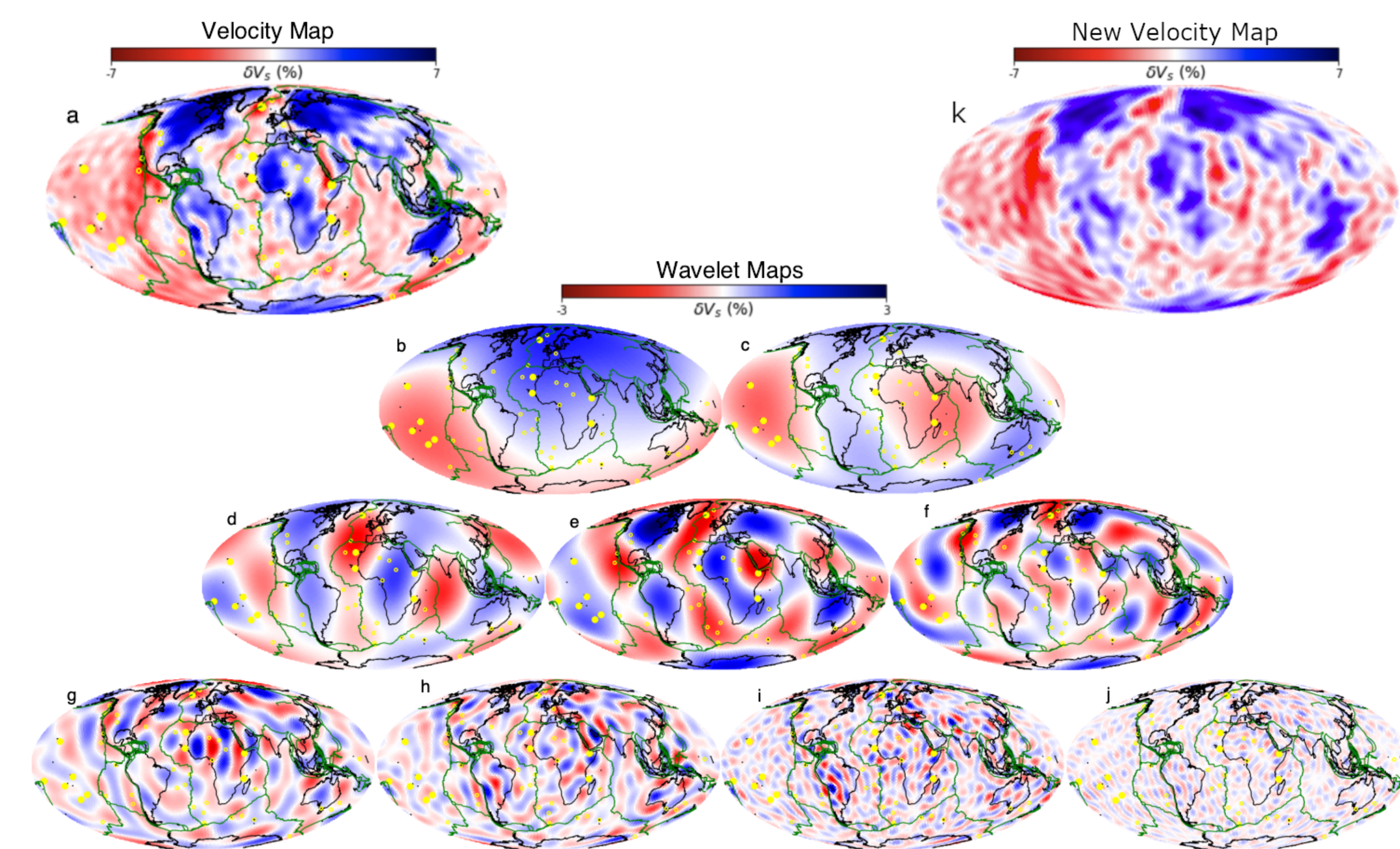


Figure 1: SGLLOBE-rani at 200 km depth (a) and its spherical wavelet transform (b-j). An example new velocity map made by simulating scales i-j is shown in k. We use the scale-discretised axisymmetric wavelet transform of Leistedt et al. (2013).

## Plume Probabilities

Each map at a depth  $z$  is tiled by an  $8^\circ \times 8^\circ$  grid. In each tile we calculate the signal-to-noise ratio by

$$S_z = \frac{1}{N} \sum_{i=1}^N \frac{\delta v_{s_i}}{\sigma_v},$$

where  $N$  is the number of maps,  $\delta v_{s_i}$  is the velocity perturbation in the  $i^{\text{th}}$  map and  $\sigma_v$  is the standard deviation of the maps. The probability of a plume in a tile is then defined as

$$P(\text{plume}) = \int_{-\infty}^{\infty} \frac{1}{N_z} \sum_{z=1}^{N_z} \frac{1}{2\pi\sigma_z} \exp\left\{-\frac{(S_z - \mu_z)^2}{\sigma_z^2}\right\} dS_z,$$

where  $\mu_z$  and  $\sigma_z$  are the mean and standard deviation of  $S_z$ , and  $N_z$  is the number of depths. We also define a confidence  $n$ , which measures how negative the mean of the distribution of  $S$  is. A more negative mean, larger  $n$ , represents a higher confidence.

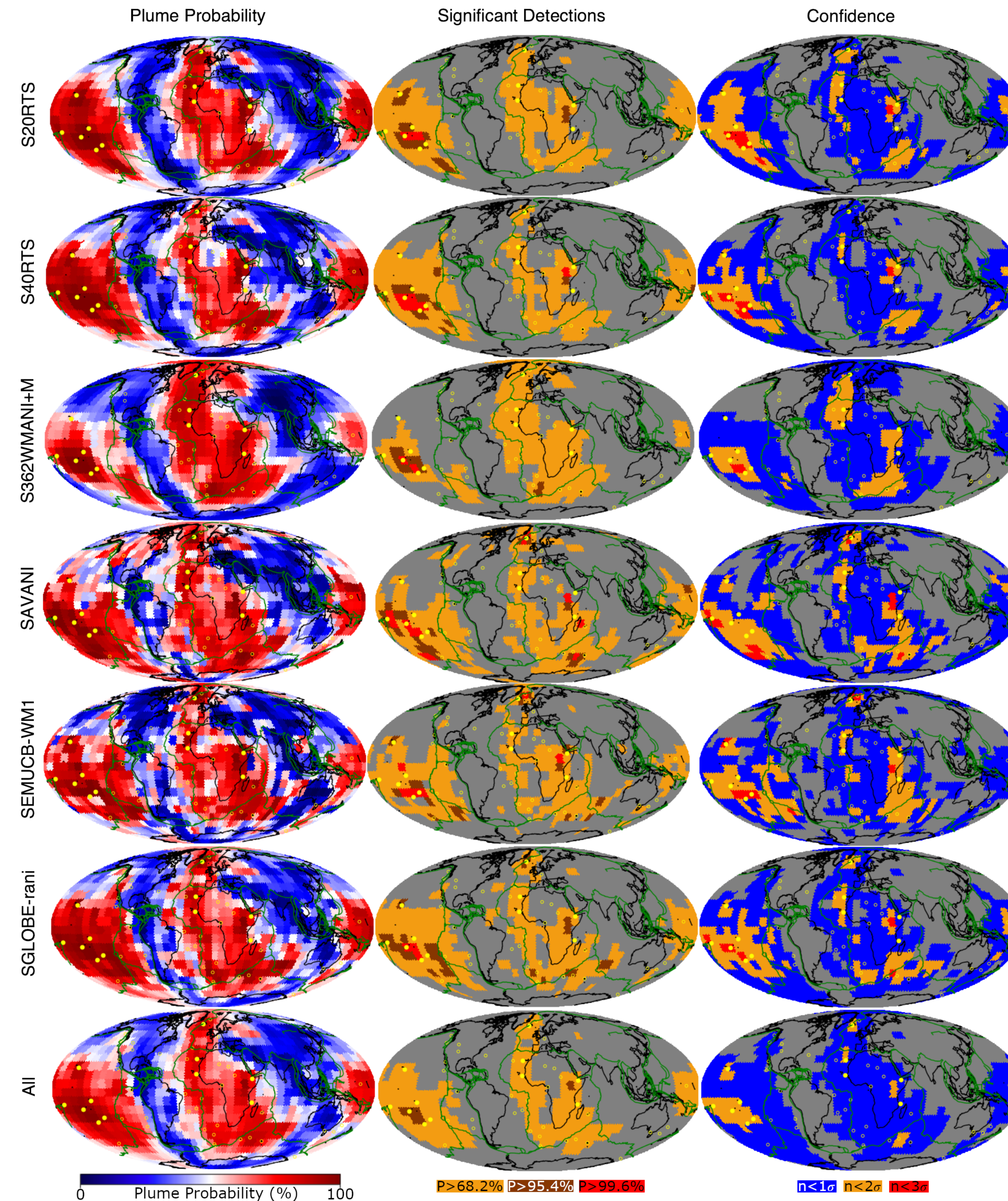


Figure 2: Left column - Plume probability maps. Middle Column - Probabilities greater than 66.2%, 95.4% and 99.6%. Right column - Confidence in plume probability. Filled yellow circles are the 11 primary plumes of French and Romanowicz (2015). Empty circles are other hotspots (Courtilot et al., 2003).

Plume	S20RTS	S40RTS	S362WMANI+M	SAVANI	SEMUCB-WM1	SGLLOBE-rani
Afar	92.13	93.68	73.78	58.40	95.81	83.11
Canaries	91.94	88.93	87.43	90.69	76.12	91.38
Cape Verde	79.09	78.40	83.42	84.86	79.24	83.54
Comoros	50.22	55.09	79.24	86.62	87.82	61.22
Hawaii	92.42	91.31	54.95	79.29	99.09	98.49
Iceland	70.82	85.13	79.99	100	91.66	97.27
Macdonald	99.04	99.99	99.94	99.66	100	99.85
Marquesas	98.91	95.52	93.39	82.71	90.97	88.55
Pitcairn	99.48	99.98	97.85	94.13	100	95.32
Samoa	95.13	93.04	76.48	99.22	81.03	97.28
Tahiti	99.98	100	99.64	100	93.85	100

Table 1: Plume probabilities at the 11 primary plume locations of French & Romanowicz (2015).

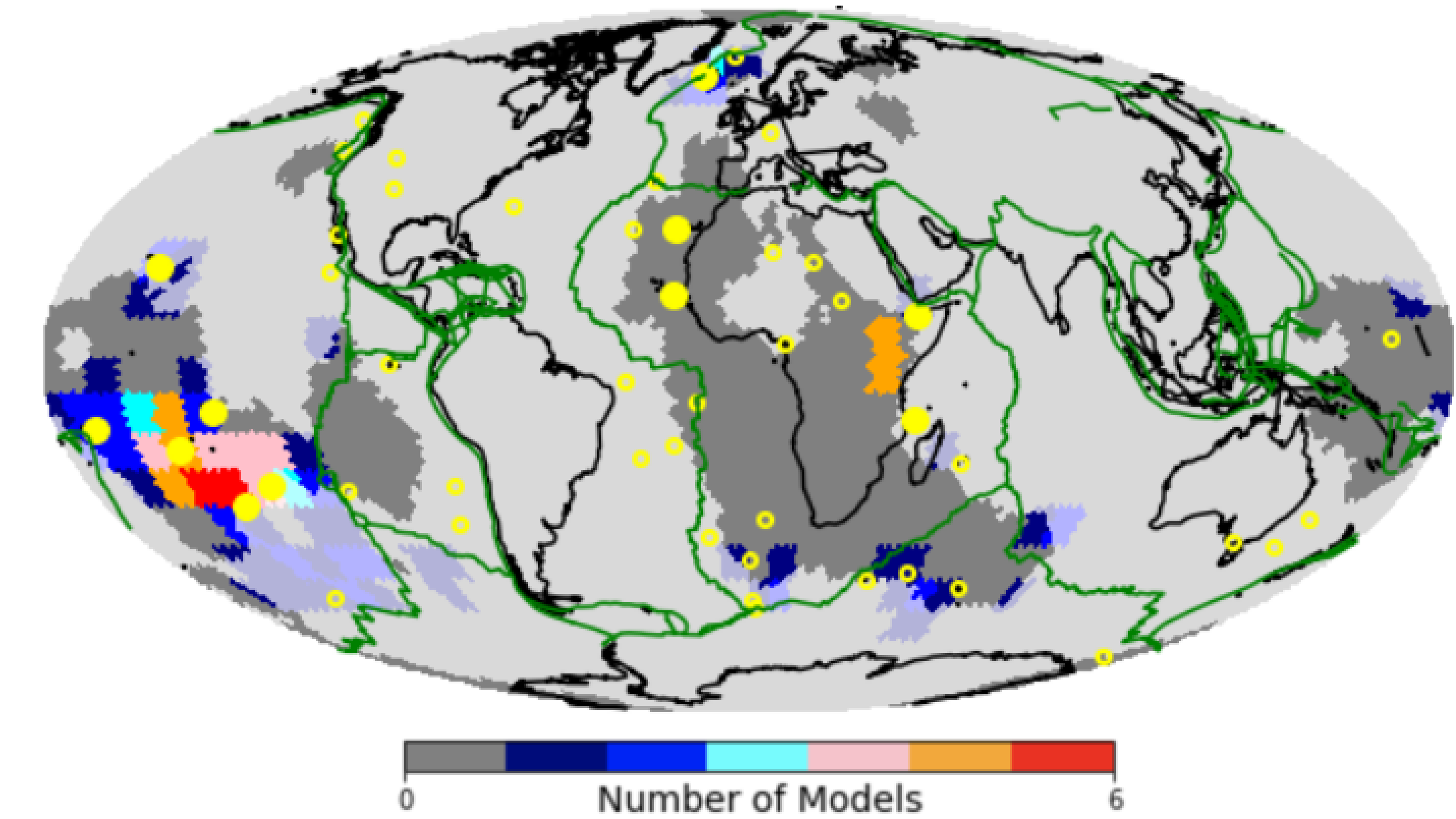


Figure 3: Vote map of very high probability plumes. Each model assigns one vote to a tile when the plume probability is greater than 95%. Darker shades show the LLSVPs from Cottaar & Lekic (2016). Filled yellow circles are the 11 primary plumes of French and Romanowicz (2015). Empty circles are other hotspots (Courtilot et al., 2003).

## Correlation with LLSVPs

Probability maps show high probabilities under the Pacific and Africa, so we look for a correlation between plume probability and shear wave velocity. Figure 4 shows the correlation between probability and velocity maps at depth beneath, and outside, the African and Pacific LLSVPs.

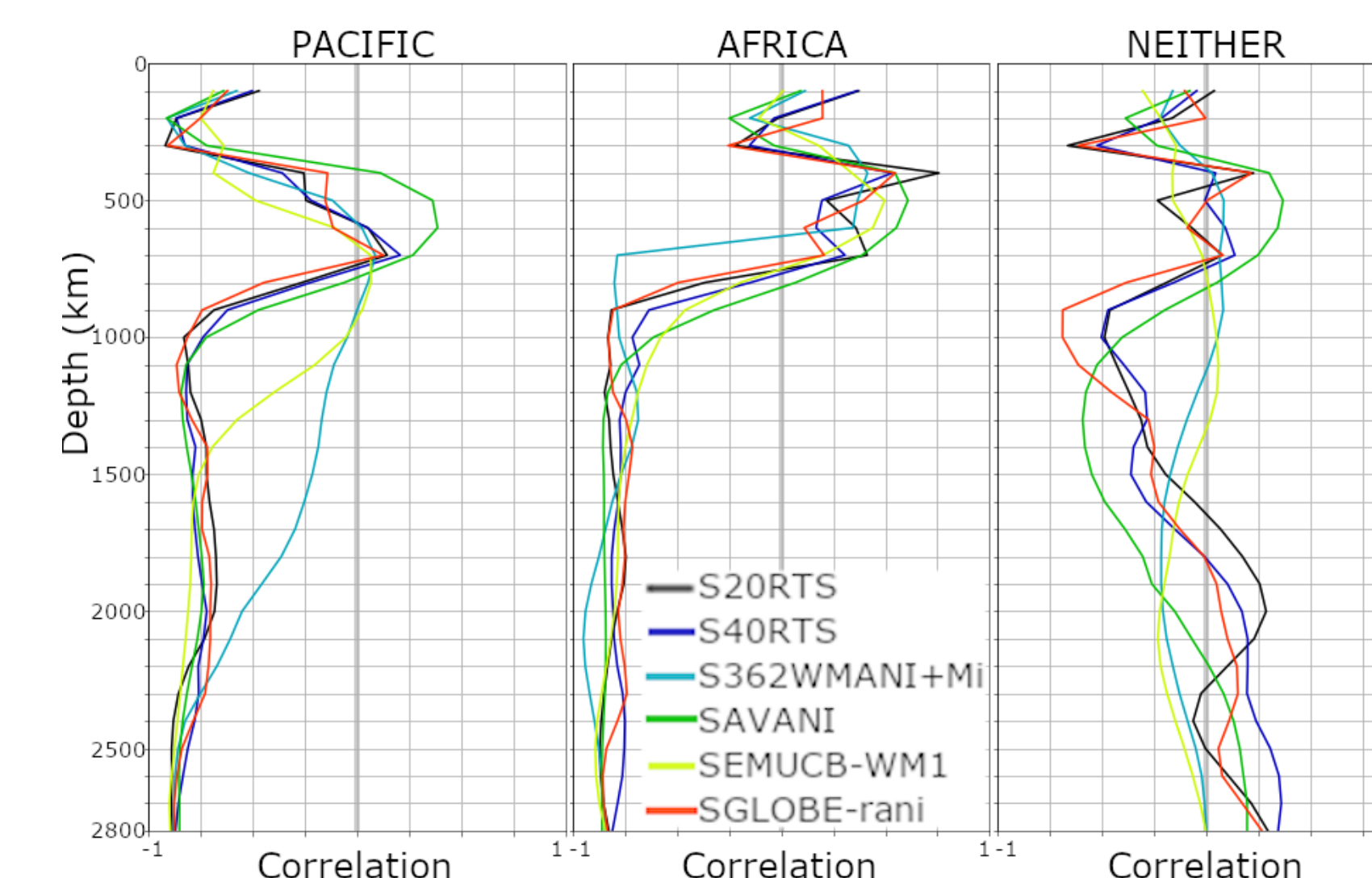


Figure 4: Correlation coefficients between probability and velocity maps depth within the boundaries of LLSVPs given by Cottaar & Lekic (2016). Correlation is calculated by

$$C = \frac{1}{N_p} \sum_p \frac{P(\text{plume})(p) \langle \delta v_s \rangle (p)}{P(\text{plume})_{rms} \langle \delta v_s \rangle_{rms}},$$

where  $p$  is a point in the LLSVP of interest.

## Conclusions

- We have developed an automated method for assessing the probability of mantle plumes in tomographic models.
- Regions of high plume probability are found beneath Kenya and southern Pacific.
- All 11 primary plumes from French & Romanowicz (2015) have greater than 50% probability in all the models, though few have a consistently high probability.
- Correlations are observed between probability and velocity maps at the LLSVPs.

## References

Auer et al., 2014, *JGR:SE*. Chang et al., 2015, *JGR:SE*. Cottaar & Lekic, 2016, *GJI*. Courtilot et al., 2003, French & Romanowicz, 2014, *GJI*. French & Romanowicz, 2015, *Nature*. Leistedt et al., 2013, *AGU*. Lekic et al., 2012, *EPSL*. Marignier et al., (*in prep*). Moulik & Ekström, 2014, *GJI*. Ritsema et al., 2004, *JGR*. Ritsema et al., 2011, *GJI*.